

# CALCULATION OF FLOW AND BED DEFORMATION IN COMPOUND CHANNEL WITH VERTICAL DROP SPILLWAYS

by

Yasuyuki Shimizu

Associate Professor, Graduate School of Engineering,  
Hokkaido University, Sapporo, Japan

## SYNOPSIS

Compound channel with a series of vertical drop spillways in the low water channel is a popular countermeasure for flood and sediment control works in Japan, especially in rivers with steep slopes. The Toyohira River, the main river flowing through the city of Sapporo, has eight low head dams in the low water channel with every several hundred meters downstream. It is desired, from an engineering standpoint, to evaluate the hydraulic function, effects and existing problems in such compound channel rivers. In this paper, a numerical model to simulate flow and bed deformation in compound channel with a series of vertical drop spillways is developed. Calculated results are compared with the results obtained in moveable bed experiments.

*Key words: compound channel, vertical drop spillway, numerical model.*

## INTRODUCTION

Vertical drop spillways are common powerful countermeasures to prevent bed erosion of alluvial rivers. They are often installed successively along river courses when the channel course has been changed, such as after cutoff works of a meandering channel. Figure 1 is a photo of the Toyohira River which flows through the center of Sapporo city. Between 1950 and 1973, eight vertical drop spillways were constructed [Ishikari river development and construction office (1)]. These structures made a great contribution to stabilize the channel bed. However, the river bed slope is still very steep in this reach and thus the velocity during the flood becomes as rapid as 10m/s and erosion is still a serious problem, as shown by Yamashita et al. (2). There is an argument that these structures should be rebuilt to reduce the velocity. The Toyohira River is also a very important river for recreational use. Therefore, it is important to study the hydraulic function of the vertical drop spillways and clarify the problems under the present conditions.

Figure 1 shows alternate bars are dominant in the low water channel, and they still remain while passing through the spillways. Besides alternate bars and vertical drop

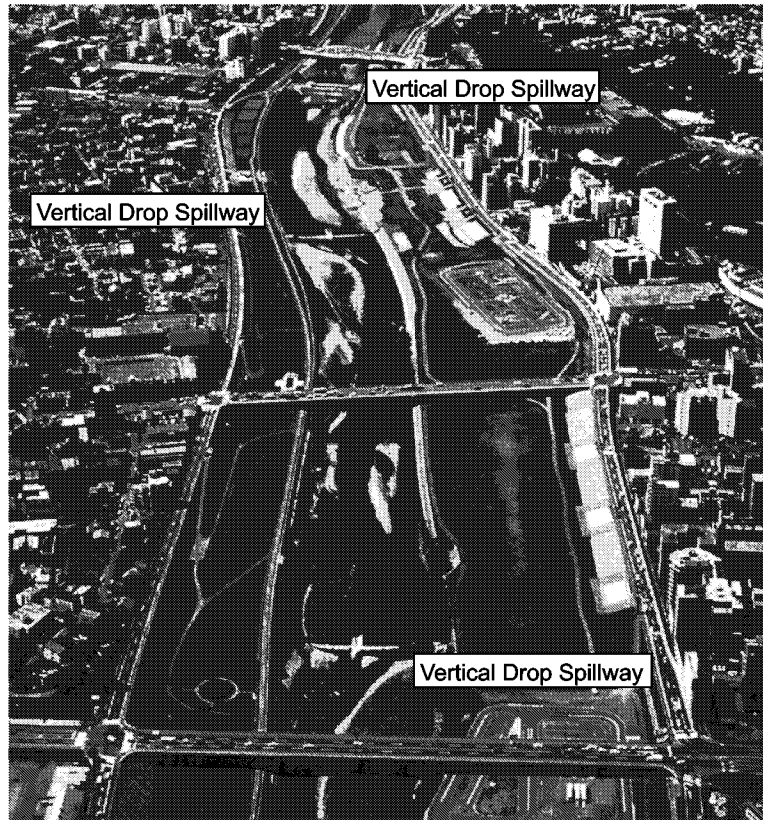


Figure 1: **The Toyohira River** (View from downstream, by Ishikari River Development and Construction Office)

spillways, some other complicated conditions coexist in the Toyohira River; The channel is compound, flow is rapid, sediment transport is very active. Therefore, the hydraulic function of the Toyohira River has to be studied from many angles. These items have been studied individually by many researchers. Especially, recent developments of numerical models enables to predict the flow and bed deformation including vertical drop spillways as proposed by Kawashima and Fukuoka (3) and Fukuoka et al (4). However, it is not clear if these numerical models can be applied to the Toyohira River in which many other problems coexists. It is important to investigate the applicability of numerical models from an engineering standpoint.

In this paper, a numerical method is proposed to calculate the flow and bed deformation in compound channels with vertical drop spillways. The basic equations used in this model are the two-dimensional shallow water equations which have succeeded in predicting the finite amplitude of bar formation in alluvial rivers. However, previous numerical methods such as upwind schemes are not effective when the channel has vertical drop structures and its cross-section is compound. The CIP (Cubic-Interpolated Pseudoparticle) method proposed by Yabe (5) is introduced to calculate the flow with abrupt change due to vertical drop spillways and compound channel. The model is verified through the comparison with flume experiments. The results for the two kinds of experimental conditions, bankfull flow and overbank flow, are compared with the results by the proposed mathematical model.

## BASIC EQUATION AND NUMERICAL METHOD

The two-dimensional flow field is calculated using the following continuity equation and momentum equations.

$$\frac{\partial h}{\partial t} + \frac{\partial(uh)}{\partial x} + \frac{\partial(vh)}{\partial y} = 0 \quad (1)$$

$$\frac{\partial uh}{\partial t} + \frac{\partial(u^2h)}{\partial x} + \frac{\partial(uvh)}{\partial y} = -gh \frac{\partial H}{\partial x} - \frac{\tau_x}{\rho} + h\nu_t \nabla^2 u \quad (2)$$

$$\frac{\partial vh}{\partial t} + \frac{\partial(uvh)}{\partial x} + \frac{\partial(v^2h)}{\partial y} = -gh \frac{\partial H}{\partial y} - \frac{\tau_y}{\rho} + h\nu_t \nabla^2 v \quad (3)$$

in which  $x$  and  $y$  are orthogonal coordinates,  $u$  and  $v$  are depth averaged velocity components in  $x$  and  $y$  directions, respectively,  $h$  is flow depth,  $H$  is water surface elevation ( $=h+\eta$ ),  $\eta$  is bed elevation,  $\tau_x$  and  $\tau_y$  are bed shear stress in  $x$  and  $y$  directions, respectively,  $\nu_t$  is kinetic eddy viscosity,  $\rho$  is water density, and  $g$  is acceleration due to gravity.  $\tau_x$  and  $\tau_y$  can be expressed using Manning's equation as;

$$\frac{\tau_x}{\rho} = \frac{gn^2 u \sqrt{u^2 + v^2}}{h^{1/3}}, \quad \frac{\tau_y}{\rho} = \frac{gn^2 v \sqrt{u^2 + v^2}}{h^{1/3}} \quad (4)$$

in which  $n$  is Manning's roughness coefficient.  $\nu_t$  is given by the following equation.

$$\nu_t = \frac{\kappa}{6} u_* h \quad (5)$$

in which  $\kappa$  is the von Karman constant and  $u_*$  is shear velocity, calculated by

$$u_*^2 = \frac{gn^2(u^2 + v^2)}{h^{1/3}} \quad (6)$$

Time dependent change of bed elevation is calculated by the following continuity equation of sediment transport.

$$\frac{\partial \eta}{\partial t} + \frac{1}{(1-\lambda)} \left[ \frac{\partial q_{bx}}{\partial x} + \frac{\partial q_{by}}{\partial y} \right] = 0 \quad (7)$$

in which  $\lambda$  is porosity of bed material,  $q_{bx}$  and  $q_{by}$  are bed load sediment transport rate per unit width in  $x$  and  $y$  directions, which are calculated by M.P.M. formula and Hasegawa's formula (6), respectively.

$$\frac{q_{bx}}{\sqrt{\left(\frac{\rho_s}{\rho} - 1\right)gd^3}} = 8(\tau_* - \tau_{*c})^{3/2} \quad (8)$$

$$q_{by} = q_{bx} \left( \frac{v}{u} - N_* \frac{h}{r_*} - \sqrt{\frac{\tau_{*c}}{\nu_s \nu_k \tau_*}} \frac{\partial \eta}{\partial y} \right) \quad (9)$$

in which  $\rho_s$  and  $d$  are density and diameter of bed material, respectively,  $\tau_*$  is non-dimensional bed shear stress [ $=u_*^2/(sgd)$ ,  $s = \rho_s/\rho - 1$ ], and  $\tau_{*c}$  is non-dimensional critical shear stress which is calculated by Iwagaki's formula.  $\nu_s$  and  $\nu_k$  are static and kinetic friction coefficient of sand particles, respectively. The second term of right hand side of Eq. 9 acts as additional transverse sediment load when the secondary flow is developed. The flow field described in this paper is two-dimensional, however, the secondary flow

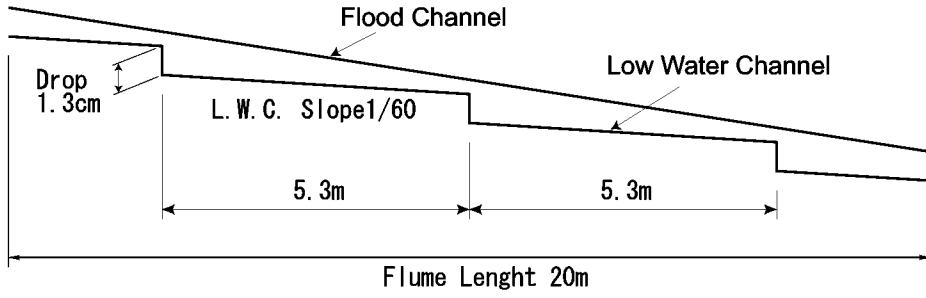


Figure 2: Longitudinal profile of experimental flume

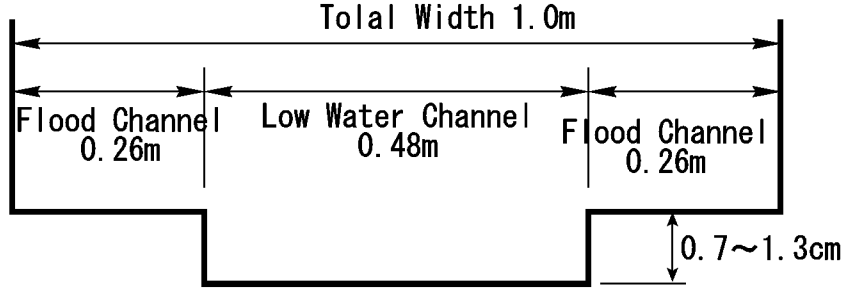


Figure 3: Cross section of experimental flume

is taken into account when the stream line is curved because of the development of a three-dimensional bed configuration. A constant value of 7 is used for  $N_*$  according to Engelund (7), and  $r_*$  is expressed by the radius of curvature of a streamline, and it is calculated by the following equation suggested by Shimizu and Itakura (8).

$$\frac{1}{r_*} = \frac{1}{(u^2 + v^2)^{3/2}} \left\{ u \left( u \frac{\partial u}{\partial x} - v \frac{\partial v}{\partial x} \right) + v \left( u \frac{\partial v}{\partial y} - v \frac{\partial u}{\partial y} \right) \right\} \quad (10)$$

In solving momentum equations (Eqs. 2 and 3), a solution technique is used, in which equations are separated into two phases of advection and non-advection. The CIP method is used for advection phase, while SOR method is used to calculate the non-advection phase of momentum equations coupled with continuity equation of Eq. 1. CIP method is originally proposed by Yabe (5) and modified for the calculation of open channel flow by Nakayama et al. (9). Time dependent change of bed elevation is computed by Eq. 7 using central finite differences.

## MOVEABLE BED EXPERIMENTS

Experiments were conducted in a flume with a compound cross-section and vertical drop spillways. Figure 2 and 3 show the outline of the experimental flume. The length and width of the flume are 20m and 1m, respectively. The central part of the channel is a low water channel with 48cm width. The low water channel bed is covered with uniform grain size sand of 0.2mm diameter. The flood channels on both sides are made of mortar. Along the low water channel, three vertical drop structures are installed in every 5.3m interval. The vertical drop of each structure is 1.3cm. The experimental set up was designed to simulate a 1/50 scale model of the Toyohira River. Two series of experiments were conducted for bank-full and over-bank flows. Discharges of 2ℓ/sec and 7 ℓ/sec were

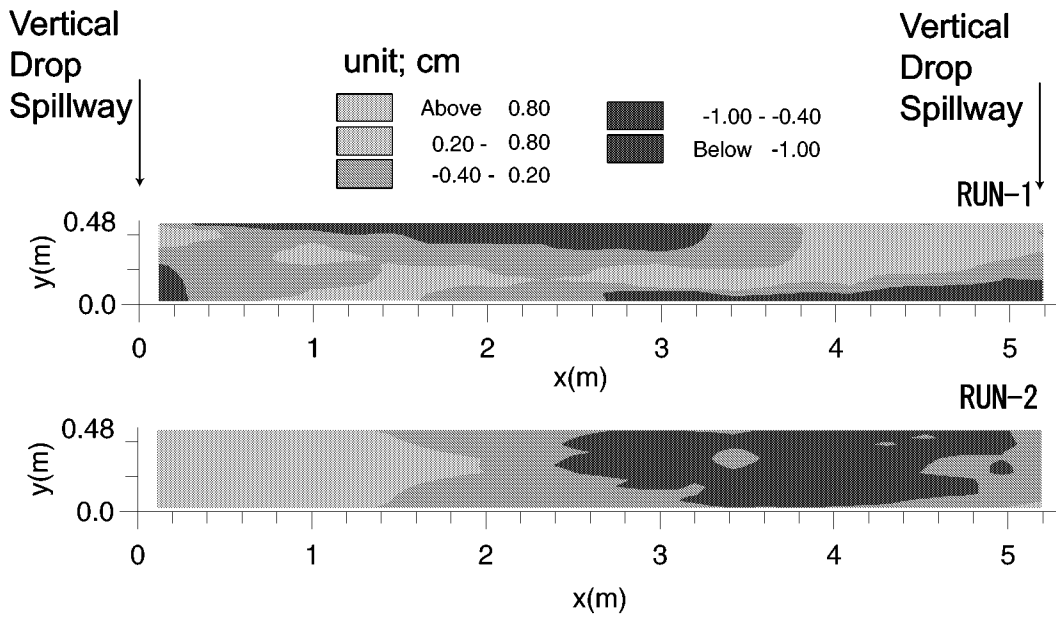


Figure 4: Bed elevation deviation contour of experiment

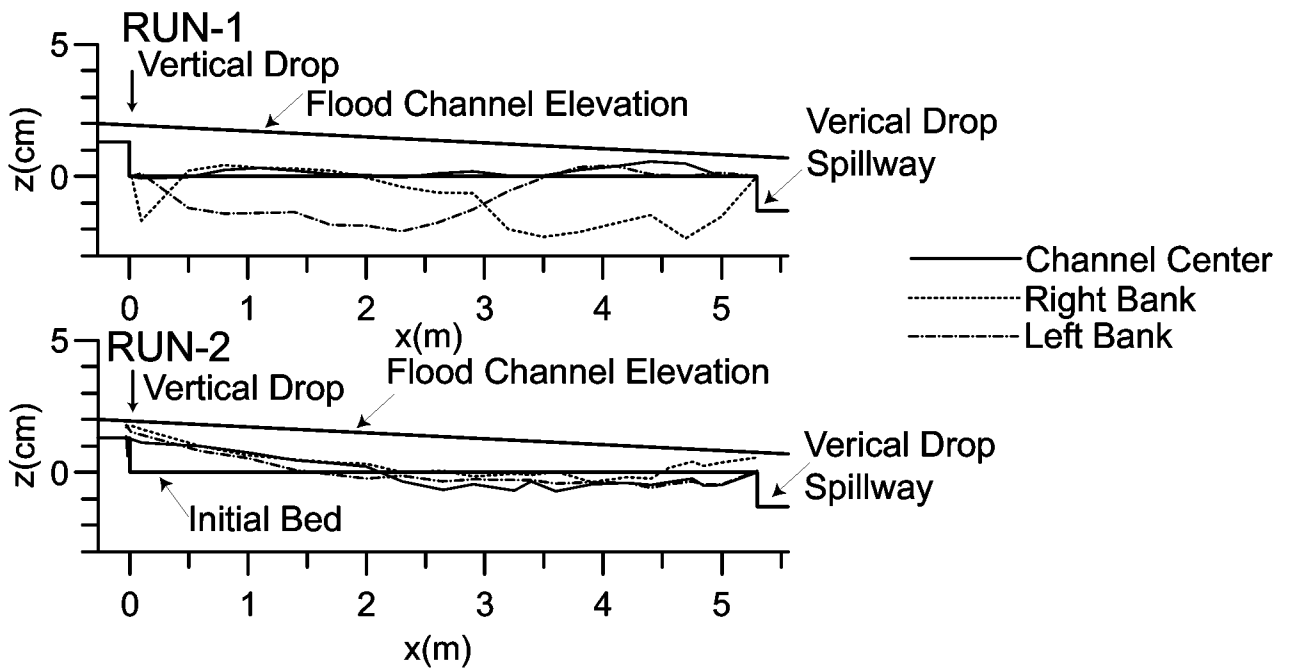


Figure 5: Longitudinal bed elevation profile of experiment

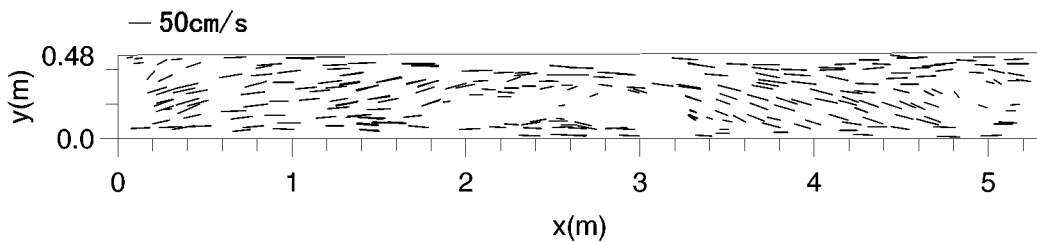


Figure 6: Velocity vector of experiment

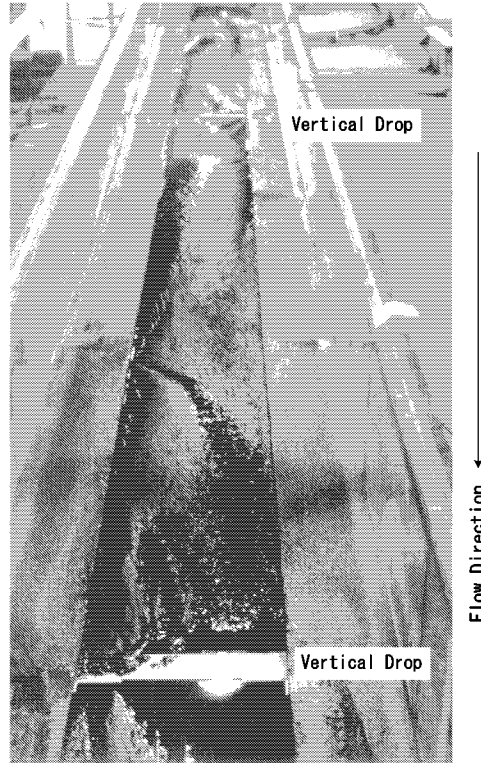


Figure 7: **Photo of Channel Bed (RUN-1, After Experiment)**

chosen for RUN-1 and RUN-2, respectively. Experiments were continued about an hour until the bed elevation reached the equilibrium state. Sediment was supplied keeping the bed elevation at upper end of the flume constant. At the end of RUN-1, the surface velocity was measured by PIV technique with styrofoam grains as tracers. Almost identical bed configuration between the adjacent vertical drop structures was formed in both experiments.

Figure 4 shows the bed configuration (deviation from initial bed), and Figure 5 shows the bed elevation profile in the downstream direction. Figure 6 shows the surface velocity vectors at the final stage of RUN-1 measured by PIV technique.

In RUN-1, as the low water channel bed was most eroded at the downstream of vertical drop and it became shallower along the channel, overflow to the flood channel started about 2m upstream of the vertical drops. Flooded water came back to the low water channel after the vertical drop. This behavior is often observed during the snow melting season in the Toyohira River. Migrating alternate bars were observed during the experiment RUN-1. Figure 7 shows the picture of alternate bars taken after the experiment RUN-1.

Alternate bars were not recognized after RUN-2. The averaged hydraulic conditions of the two cases, was plotted in a diagram proposed by Kuroki and Kishi (10) as shown in Figure 8. Condition of alternate bar in each experiment agreed with the regime criteria of the diagram.

## NUMERICAL CALCULATION

Calculations were conducted with the same condition of the experiments described in the previous section. Manning's roughness coefficient for the moveable low water channel bed

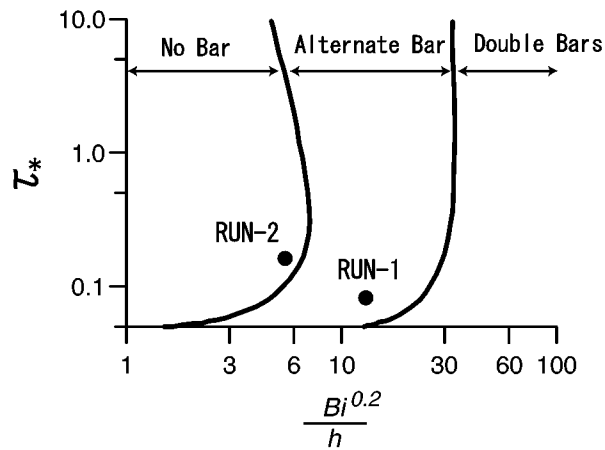


Figure 8: Regime criteria of meso-scale bar

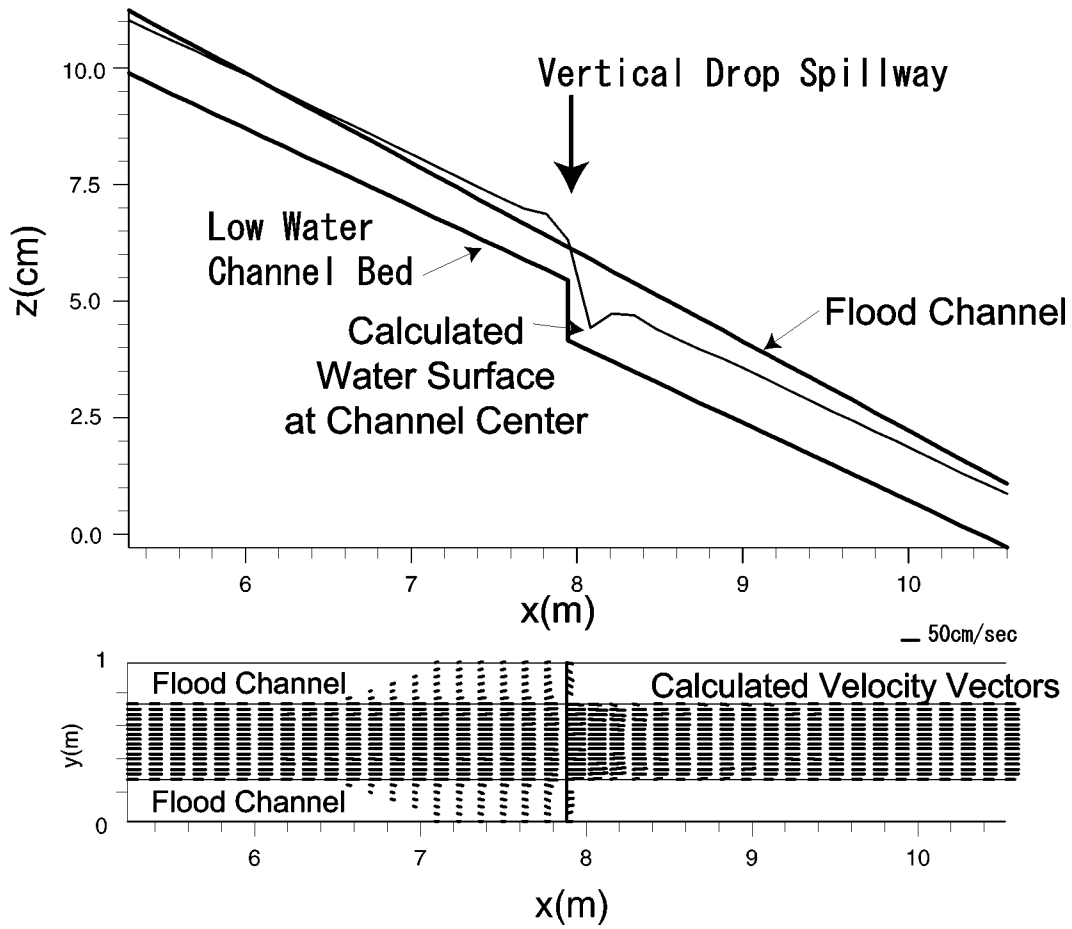


Figure 9: Calculated results of water surface elevation and velocities (RUN-1, initial bed condition)

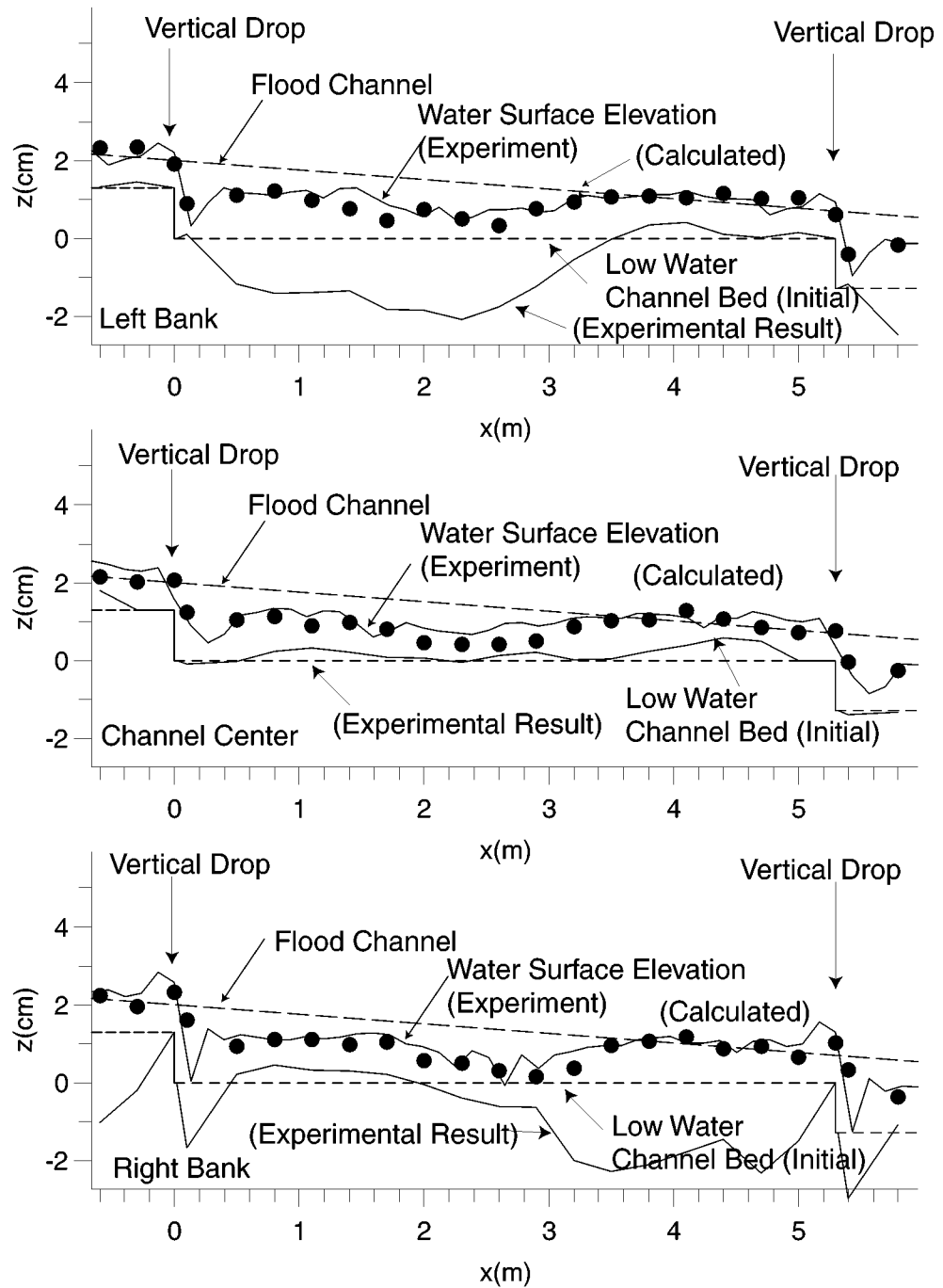


Figure 10: Comparison of observed and calculated water surface elevation



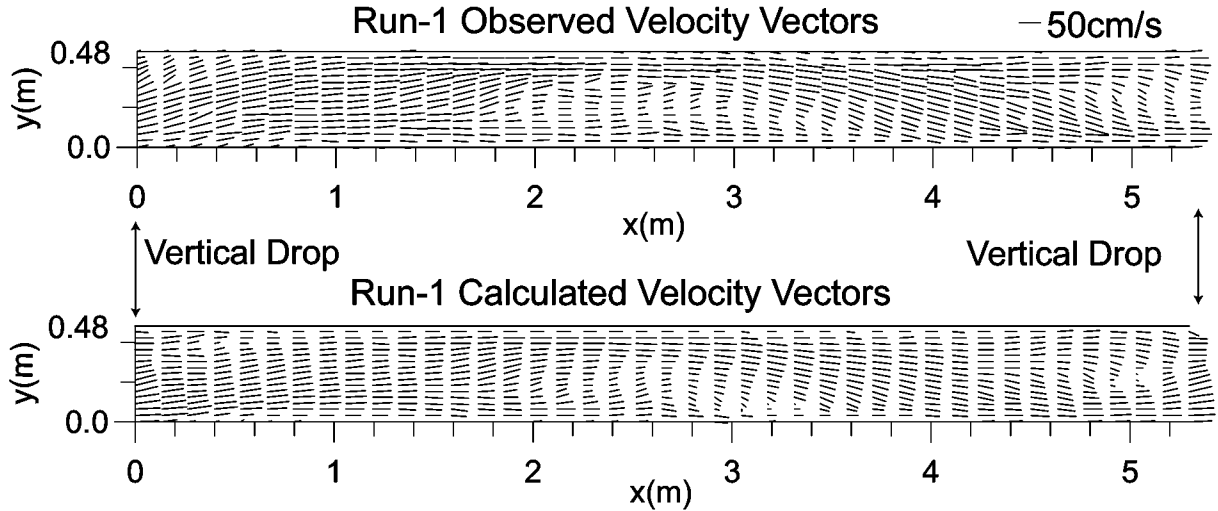


Figure 11: Comparison of velocity vectors between observed and calculated

was determined using a formula proposed by Kishi and Kuroki (10) for flat beds, and a constant value of 0.01 was used for the high water channel. Computational grids in the longitudinal and transverse directions were 122 and 28, respectively. The time step for computation was set to be 0.01 second. At the grid points on the vertical drop spillways, where the bed was fixed, calculation of bed elevation change was simply omitted.

Figure 9 shows the calculated profile of water surface elevation and velocity vectors under the initial conditions of RUN-1. The flow pattern of partial flooding around the vertical drop spillways observed in RUN-1 was well reproduced. In order to examine the accuracy of the flow calculation, the observed bed elevation after RUN-1 was given and the flow calculation of RUN-1 was conducted with fixed bed conditions. Calculated results of water surface and velocity vectors were compared with the observed ones as shown in Figures 10 and 11. They show good agreements and thus the accuracy of the flow calculation of the proposed model was verified.

Next, the performance of alternate bar formation was studied using the flow conditions of RUN-1. Calculations without vertical drop spillways were also conducted to compare the effect of vertical drop spillways. Calculations with and without spillways were continued for two hours when the bed configuration reached equilibrium. Figure 12 and 13 show the calculated bed elevation contour with and without spillways, respectively, from 3,600 seconds to 5,400 seconds in the calculation. Figure 12 shows that alternate bars are migrating downstream at constant speed. The calculated wave length of alternate bars was about 12 times of the channel width, and bar height was about 1.3cm. The calculated bar height was about 1.5 times the averaged water depth slightly smaller than that of observed value of RUN-1 shown in Figure 4. On the contrary, the well-regulated bar migration was not produced in the calculation with spillways as shown in Figure 13. It was shown that, when the bar front was approaching to the vertical drop spillways, the migration speed slowed down, and thus the regulated migration was interrupted. The calculation overestimates the deposition rate downstream of the drops. It may be caused by non-equilibrium sediment transport passing through the vertical drop spillways, which was not taken into account in the present model.

Calculation was also conducted under the condition of RUN-2, and calculated bed

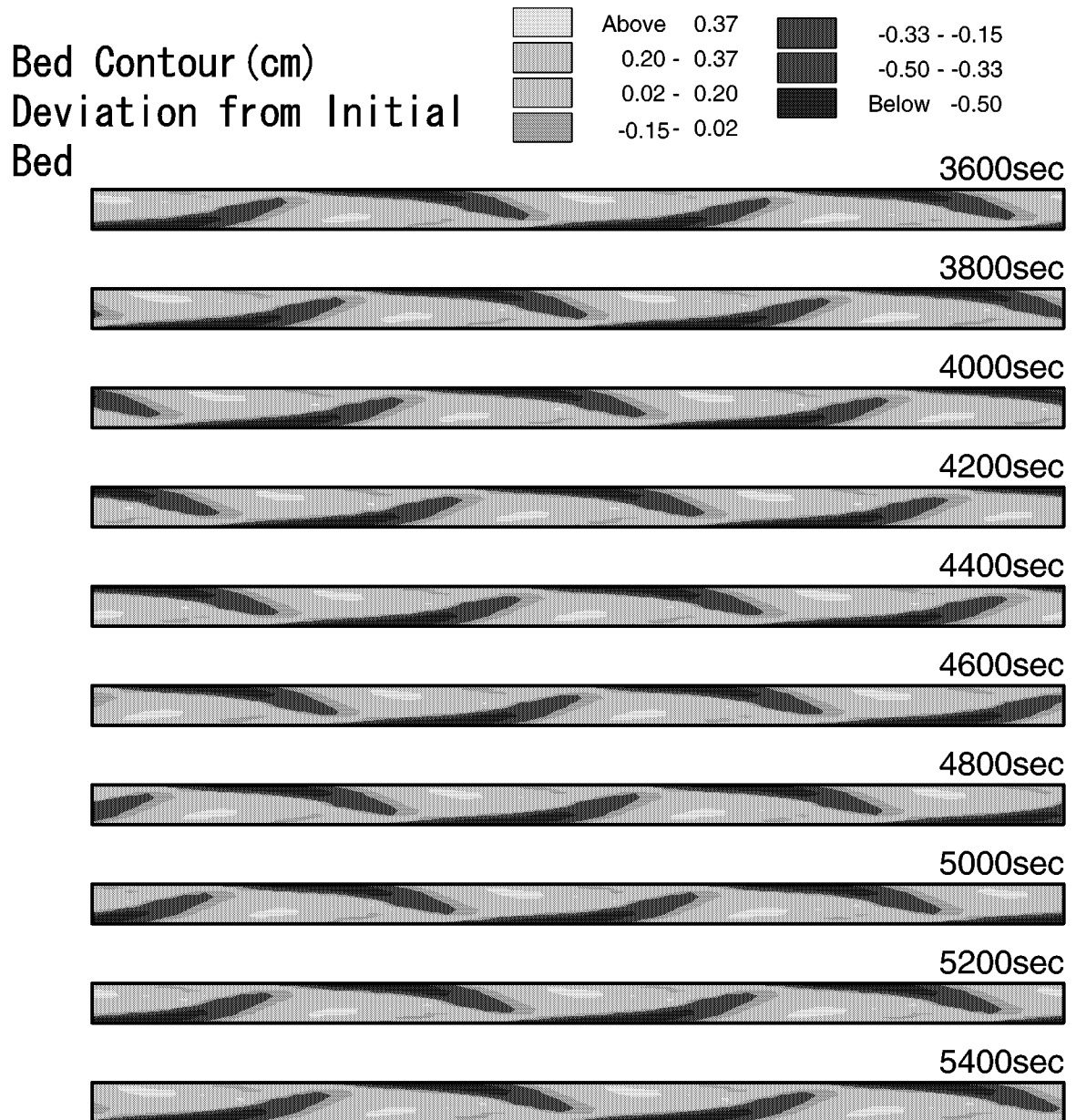


Figure 12: Calculated bed elevation (without vertical drop structures).

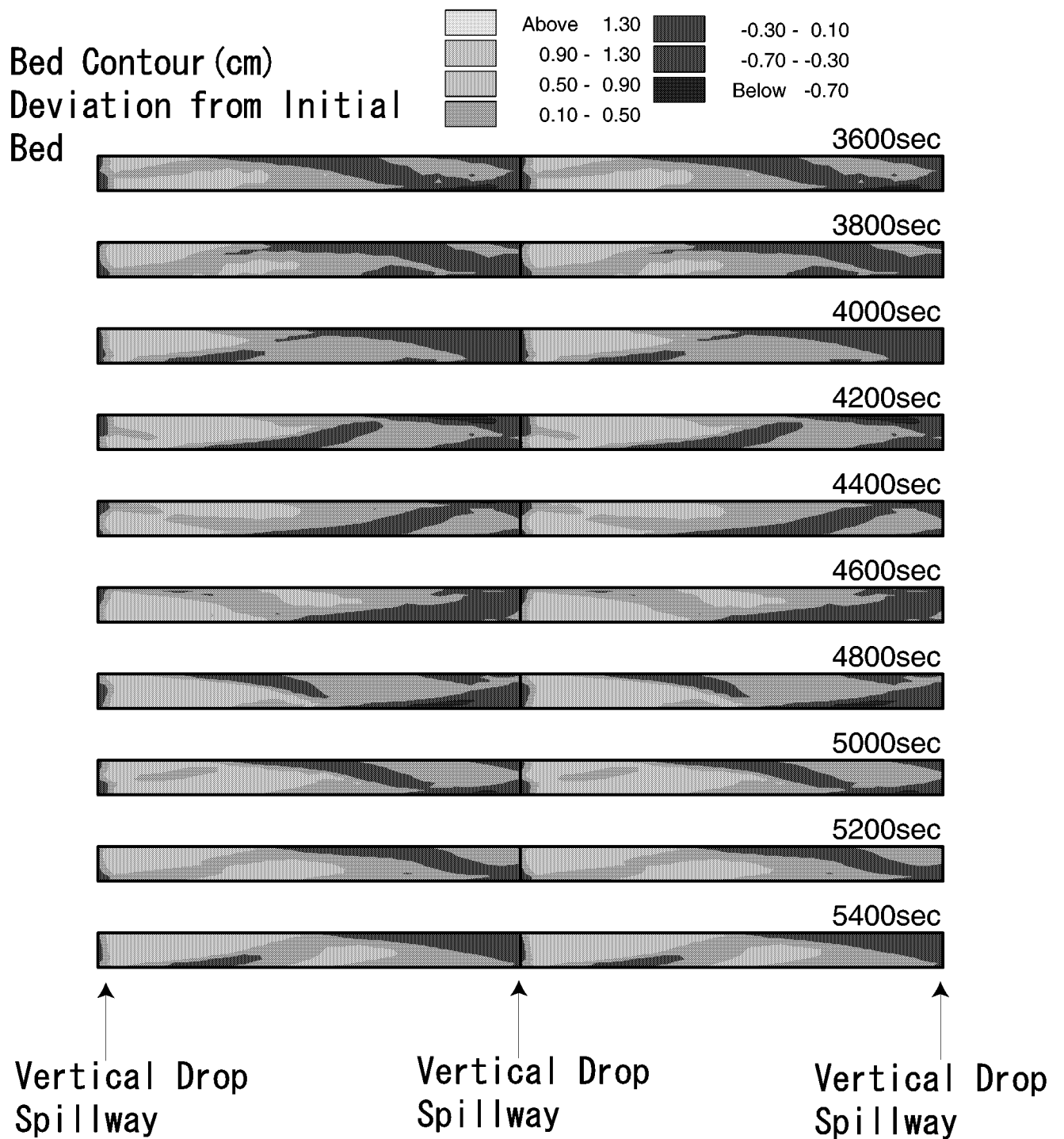


Figure 13: Calculated bed elevation changes [Run1](with vertical drop spillways)

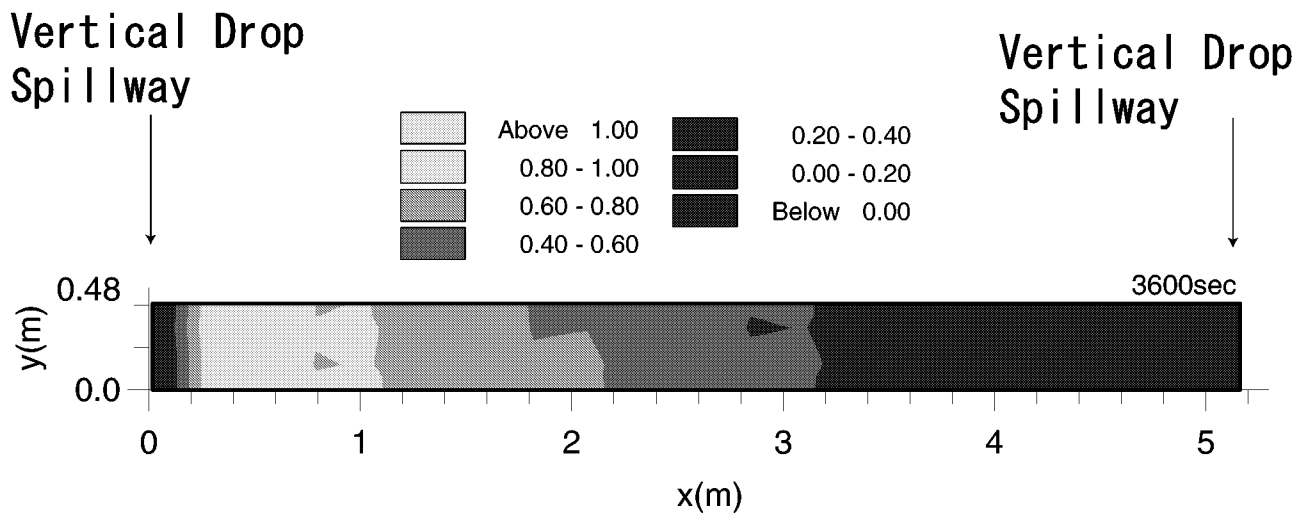


Figure 14: Calculated bed elevation changes [Run2](with vertical drop spillways)

contours are shown in Figure 14. Alternate bars are not developed in this case, which agrees with the experimental results shown in Figure 4.

## CONCLUSION

Characteristics of flow and bed deformation especially focused on bar formation were studied by flume experiments and numerical calculation. It was shown that the regime criteria for the formation of alternate bar is valid even for the case that vertical drop spillways are placed.

A numerical model was proposed to calculate the flow and bed deformation in compound channel with vertical drop spillways. In the numerical model, CIP method was introduced to calculate the flow with abrupt change by vertical drop and partially flooded compound channel. The applicability of the model was confirmed through the comparison with the experimental results. The condition of examples shown in this paper was considered impossible to be applied by the existing models. However, the performance of the proposed model by coupling with the CIP method was very successful.

## REFERENCES

- (1) Ishikari River Development and Construction Office: 20 years history of Ishikari River Construction Office, pp. 1-271, 1993 (in Japanese).
- (2) Yamashita, S. , Shimizu Y., and Watanabe Y.: River bed deformation around vertical drop spillways in steep rivers, Annual Journal of Hydraulic Engineering, JSCE, Vol.36, pp.87-96, 1992 (in Japanese).
- (3) Kawashima, M. and Fukuoka, S.: A study on a numerical calculation method including bed protection works, Annual Journal of Hydraulic Engineering, JSCE, Vol.39, pp.689-694, 1995 (in Japanese).

- (4) Fukuoka, S., Watanabe, A. and Okada, S: Analysis of bed deformation in compound meandering channel with hydro-static assumption, Annual Journal of Hydraulic Engineering, JSCE, Vol.42, pp.1015–1020, 1998 (in Japanese).
- (5) Yabe, T. and Ishikawa, T.: A Numerical Cubic-Interpolated Pseudoparticle(CIP) Method without Time Splitting Technique for Hyperbolic Equations, Journal of the Physical Society of Japan, Col.59, No.7, pp.2301-2304, 1990.
- (6) Hasegawa, K. and Yamaoka, S.: The Effect of plane and bed forms of channels upon the meander development, Journal of Hydraulic, Coastal and Environmental Engineering, JSCE, Vol229, pp.143–152, 1980. (in Japanese).
- (7) Engelund, F.: Flow and Bed Topography in Cannel Bends, Jour. of Hydraulic Div., ASCE, Vol.100, HY11, pp.1631–1648, 1974.
- (8) Shimizu, Y. and Itakura, T.: Calculation of flow and bed deformation with a general non-orthogonal coordinate system, Proc. of XXIV IAHR Congress, Madrid, Spain, C-2, pp.241-248, 1991.
- (9) Nakayama, K., Sato, K. and Horikawa, Y: Numerical calculation of shallow water flow using CIP method, Annual Journal of Hydraulic Engineering, JSCE, No. 42, pp.1159–1164, 1998. (im Japanese).
- (10) Kuroki, M. and T. Kishi: Regime Criteria on Bars and Braids in Alluvial Straight Channels, Journal of Hydraulic, Coastal and Environmental Engineering, JSCE, No.342, pp.87–96, 1984 (in Japanese).
- (11) Kishi. T. and Kuroki. M: Bed form and flow resistance in alluvial rivers (I), Research Report of Faculty of Engineering, Hokkaido University, No. 67, pp.1-23, 1973. (in Japanese).

## APPENDIX – NOTATION

The following symbols are used in this paper:

$d$	=	diameter of bed material;
$g$	=	acceleration due to gravity;
$h$	=	flow depth;
$H$	=	water surface elevation;
$n$	=	Manning's roughness coefficient;
$N_*$	=	7;
$q_{bx}$	=	bed load sediment transport rate per unit width in $x$ direction;
$q_{by}$	=	bed load sediment transport rate per unit width in $y$ direction;
$r_*$	=	radius of curvature of streamline;
$t$	=	time;
$u$	=	depth averaged velocity components in $x$ direction;
$u_*$	=	shear velocity;
$v$	=	depth averaged velocity components in $y$ direction;
$x$	=	longitudinal axis;
$y$	=	transverse axis;

$\eta$	=	bed elevation;
$\kappa$	=	the Von Karman constant;
$\lambda$	=	porosity of bed material;
$\tau_x$	=	bed shear stress in $x$ direction;
$\tau_y$	=	bed shear stress in $y$ direction;
$\nu_k$	=	kinetic friction coefficient of sand particles;
$\nu_s$	=	static friction coefficient of sand particles;
$\nu_t$	=	kinetic eddy viscosity;
$\rho$	=	water density;
$\rho_s$	=	density of bed material;
$\tau_*$	=	non-dimensional bed shear stress; and
$\tau_{*c}$	=	non-dimensional critical shear stress.